

Attosecond pulse trains as multi-color coherent control

J. V. Hernández and B. D. Esry

J.R. Macdonald Laboratory, Kansas State University, Manhattan, Kansas 66506

(Dated: November 3, 2018)

We present a general description of the interaction between multi-color laser pulses and atoms and molecules, focusing on the experimentally relevant example of infrared (IR) pulses overlapped with attosecond pulse trains (APTs). This formulation reveals explicitly and analytically the role of the delay between the IR pulse and APT as a coherent control parameter. Our formulation also shows the nearly equivalent roles of the delay and the carrier-envelope phase in controlling the interference between different multiphoton pathways. We illustrate these points by investigating the single ionization of He and introduce dressed adiabatic hyperspherical potentials to aid the discussion. We confirm the predictions with a full-dimensional, two-electron solution of the time-dependent Schrödinger equation.

PACS numbers: 32.80.Rm,42.50.Hz

At the heart of atomic and molecular physics is the motion of bound electrons. Since the relevant time scale for their motion is on the order of atomic units (1 a.u. \approx 24 as), detailed studies of electron dynamics require forces that act on these time scales. With such forces, an avenue for control over the electron dynamics is also created. These abilities to study and control are the central goals of the nascent field of laser-based attosecond physics [1, 2].

Attosecond pulses are generated experimentally via high-harmonic generation, either as a single isolated pulse [3] or as an attosecond pulse train (APT) [4]. The latter, which we will focus on in this Letter, contains a large range of harmonics of the fundamental infrared (IR) laser (usually a Ti:Sapphire at approximately 800 nm). With selective filtering, a specific range of harmonics — typically in the extreme ultraviolet range — can be isolated and used to illuminate the target. Temporally, these harmonics combine to give a periodic series of pulses, each of which is an attosecond pulse, thus the label APT. When overlapped with an IR pulse, an APT permits control through the ability to vary the delay between the APT and IR field which can be done on a tens-of-attoseconds scale. Experimental control of the ionization probability using such a method has been realized [5, 6], as has control over the angular distribution [7, 8].

Electron dynamics in the combined IR+APT field can, of course, be described by solving the time-dependent Schrödinger equation [9]. To try to gain some physical insight, though, both a time-dependent, electric field picture [5, 10] and a time-independent, photon based picture [11, 12] have been applied. An approach akin to the “simple man’s approximation” has also been invoked to describe the dependence on delay using wave packet replicas [13].

While these attempts to understand the dynamics in IR+APT laser fields have some interpretive power, they are not general, exact, nor do they provide a simple

route to predicting the outcome of a particular experiment. The numerical solution of the time-dependent Schrödinger equation is, in principle, general and exact, but is limited in practice to simple systems and cannot be said to provide a simple guide to predictions. Thus, a rigorous description of the problem is desired that can also provide a conceptual framework within which predictions can be made simply.

In this Letter, we present just such a theoretical framework. This formulation is closely related to one we have developed [14, 15] to understand the effects of the carrier-envelope phase (CEP) for few-cycle pulses and, in fact, demonstrates that both the CEP and the IR+APT delay provide essentially identical control over a system. This conclusion follows because both of these parameters can be thought of as controlling the relative phase between different multiphoton processes that interfere to produce a given physical observable. In fact, attosecond pulses can be characterized by taking advantage of such interferences [4, 16, 17]. These systems are realizations of the canonical coherent control scenario proposed by Brumer and Shapiro [18]. Moreover, because an APT is a synthesis of harmonics, our analysis applies equally well to, and provides a connection to, the well-studied two-color experiments on controlling molecules [18, 19, 20, 21].

Rather than presenting the most general formulation of our theory — which, while conceptually simple, is notationally cumbersome — we illustrate it by applying it to the single ionization of helium by combined IR+APT fields [5]. We confirm our analysis with solutions of the full six-dimensional, two-electron, time-dependent Schrödinger equation. In the process, we thus account for the modulation in ion yield with delay between IR and APT recently observed in Ref. [5] both analytically and numerically.

Our analytic treatment begins with the time-dependent Schrödinger equation in the dipole approximation using the length gauge (atomic units are used

throughout),

$$i \frac{\partial}{\partial t} \Psi(t) = \left[H_0 - \vec{\mathcal{E}}(t) \cdot \vec{d} \right] \Psi(t), \quad (1)$$

where H_0 is the field-free Hamiltonian and \vec{d} is the dipole operator. We take into account the fundamental IR field with frequency ω and two harmonics of order n_1 and n_2 :

$$\begin{aligned} \mathcal{E}(t) = & \mathcal{E}_1(t) \cos(\omega t + \varphi_1) \\ & + \mathcal{E}_{n_1}(t) \cos(n_1[\omega(t - \tau) + \varphi_1] + \varphi_{n_1}) \\ & + \mathcal{E}_{n_2}(t) \cos(n_2[\omega(t - \tau) + \varphi_1] + \varphi_{n_2}). \end{aligned} \quad (2)$$

The latter two terms make up the APT in our example. More harmonics can be added to shorten the individual pulses in the APT without any conceptual difficulty, but three colors is the minimum needed to describe the most significant effects observed in an IR+APT experiment such as Ref. [5] and simplifies the discussion. Note that for our analysis the harmonics' pulse envelopes $\mathcal{E}_{n_i}(t)$, which represent the envelope for the whole pulse train, must be independent of the IR-APT delay τ but are otherwise arbitrary. Much like the derivation of CEP effects in [15], we note from Eq. (1) that Ψ is periodic in τ as well as in the IR CEP φ_1 . We can thus expand Ψ in both using a discrete Fourier transform,

$$\Psi(\tau, \varphi_1; t) = \sum_{ml} e^{im\omega\tau} e^{-il\varphi_1} \psi_{ml}(t), \quad (3)$$

where $\psi_{ml}(t)$ does not depend on either τ or φ_1 . Substituting this Ψ into Eq. (1) and equating coefficients of the linearly independent exponential functions, we obtain

$$\begin{aligned} i \frac{\partial}{\partial t} \phi_{ml} = & (H_0 - l\omega) \phi_{ml} - \frac{1}{2} \vec{\mathcal{E}}_1 \cdot \vec{d} (\phi_{m,l+1} + \phi_{m,l-1}) \\ & - \frac{1}{2} \vec{\mathcal{E}}_{n_1} \cdot \vec{d} (e^{i\varphi_{n_1}} \phi_{m+n_1,l+n_1} + e^{-i\varphi_{n_1}} \phi_{m-n_1,l-n_1}) \\ & - \frac{1}{2} \vec{\mathcal{E}}_{n_2} \cdot \vec{d} (e^{i\varphi_{n_2}} \phi_{m+n_2,l+n_2} + e^{-i\varphi_{n_2}} \phi_{m-n_2,l-n_2}). \end{aligned} \quad (4)$$

In these equations, we have made the additional substitution $\psi_{ml}(t) = e^{-il\omega t} \phi_{ml}(t)$ to emphasize the connection with the Floquet representation: in the limit that the pulse lengths go to infinity, Eq. (4) reduces to many-mode Floquet theory [22]. We stress that Eq. (4) is exact even for few-cycle pulses. We could further remove the harmonic phases φ_{n_i} with Fourier transforms, but that will not be necessary for the current discussion.

We have rigorously obtained a representation in which IR+APT experiments can be understood. Further, Eq. (3) shows that the CEP and IR-APT delay provide similar control over the dynamics of a system. The physical interpretation of this control as interference of different photon pathways stems from the facts that the components ϕ_{ml} oscillate with time-dependence $e^{il\omega t}$ and correlate to the photon components in the Floquet limit. Since we consider photons with different frequencies, the

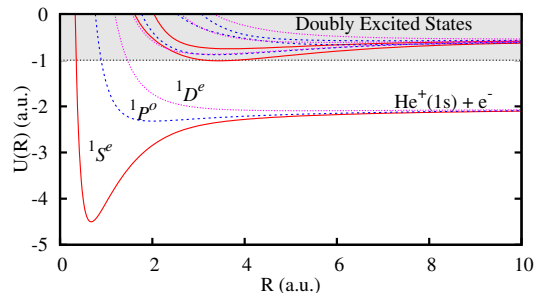


FIG. 1: (Color online) Adiabatic hyperspherical potential curves for He. Shown are $L = 0, 1, 2$ and the region of double excitation.

index l represents only the net energy $l\omega$ of the photons involved, and can be written as $l=l_1+l_{n_1}n_1+l_{n_2}n_2$ with l_i the number of photons of each color.

Specializing the above discussion to helium determines H_0 and \vec{d} in Eq. (4). We treat the full three-dimensional motion of both electrons using the adiabatic hyperspherical representation, which has proven especially useful in the past for understanding the dynamics of He [23, 24]. More specifically, we expand each component ϕ_{ml} as

$$\phi_{ml} = \sum_{L\nu} G_{mlL\nu}(R, t) \Phi_{L\nu}(R; \Omega) \quad (5)$$

where R is the hyperradius and Ω the five hyperangles. The channel functions $\Phi_{L\nu}$ solve the field-free fixed- R adiabatic equation $H_{\text{ad}}\Phi_{L\nu} = U_{L\nu}\Phi_{L\nu}$ for a given total orbital angular momentum L and thus form a complete set at each R indexed by ν . We use Delves' hyperangle and treat the system in the body frame, expanding the Euler-angle dependence of $\Phi_{L\nu}$ on Wigner D -functions (see [24] for details). The adiabatic equation thus reduces to coupled two-dimensional partial differential equations that we solve using b-splines [25].

Upon substituting ϕ_{ml} from (5) into Eq. (4) and projecting out the $\Phi_{L\nu}$ we find coupled, time-dependent equations for $G_{mlL\nu}(R, t)$ describing laser-driven motion on the adiabatic potentials $U_{L\nu}$. Since the experiments in [5] considered only single ionization at energies well below doubly-excited resonances, we can to a good approximation consider only the lowest singlet adiabatic potential $\nu=1$ for each L . These potentials support the singly-excited states $1snL \ ^1L$, and several examples are shown in Fig. 1. With this truncation of the ν expansion, we find a ground state energy of -2.895 a.u.

One advantage of using the adiabatic hyperspherical representation in the Floquet-like equations (4) is that the resulting dressed potentials — which include the effects of both Coulomb interactions and the laser field — give insight into the electronic dynamics in much the same way that Floquet potentials have for the nuclear dynamics of molecules. Applied to H_2^+ , Floquet potentials have provided natural explanations of bond-softening,

above-threshold dissociation, vibrational trapping, and zero-photon dissociation [26, 27]. Previous generalizations of the Floquet picture for H_2^+ have even helped uncover unexpected phenomena such as above-threshold Coulomb explosion [28]. It would be interesting to explore the analogues of these mechanisms for He in the present representation, but we will focus here on their application to the IR+APT case.

Figure 2 shows the diabatic dressed potentials assuming ω corresponds to 800 nm and the harmonics are $n_1=13$ and $n_2=15$ (the two most intense components of the APT in [5] by a factor of at least 5). These curves are generated by first noting that the initial state of the system, $1s^2\ ^1S^e$, has $(m,l)=(0,0)$. Then, per Eq. (4), this state couples to the $^1P^o$ channel with one IR photon $(0,\pm 1)$ or with one harmonic photon $(\pm n_i, \pm n_i)$. The $^1P^o$ potential in each case is added to the figure shifted by $l\omega$. Each of these new curves can couple to either $^1S^e$ or $^1D^e$ symmetries according to dipole selection rules, shifted in energy by an appropriate amount. Repeating this procedure, all possible multiphoton pathways combining IR and harmonic photons to any particular final state can be generated as shown in Fig. 2. The energy in such a figure can be thought of as being approximately conserved, so that the dynamics reduces to the well-understood problem of multichannel dynamics. This picture, for example, maps ionization onto predissociation of molecules in the Born-Oppenheimer approximation or, equivalently, onto atomic autoionization in the field-free adiabatic hyperspherical representation. More specifically, transitions are most likely to occur where potentials cross, and crossings of curves differing by the fewest photons will dominate. In fact, diagonalizing the right-hand-side of Eq. (4) at fixed R will produce adiabatic Floquet-like potentials in which these crossings become avoided, thus incorporating the strength of the field in the potentials themselves. The remaining time dependence in \mathcal{E}_i modulates the strength of the coupling — or the gap at the avoided crossings — as a function of time.

For the parameters above, single ionization of He requires the absorption of at least 16ω worth of energy, i.e. 16 IR photons, 1 13th harmonic plus 3 IR photons, or 1 15th harmonic plus 1 IR photons. Since it requires the fewest photons, we expect the latter scenario to be most likely, leaving the system with $(m,l)=(15,16)$ and $L=0$ or 2 based on dipole selection rules. All together, we would write these pathways as $(0,0)^1S^e \rightarrow (15,15)^1P^o \rightarrow (15,16)^1S^e$ or $^1D^e$. Following the dressed potentials in Fig. 2 suggests that only $L=2$ will be populated substantially, however, since it crosses the $(15,15)^1P^o$ curve and $L=0$ does not. The pathway beginning with the 13th harmonic would mainly proceed via $(0,0)^1S^e \rightarrow (13,13)^1P^o \rightarrow (13,16)^1D^e$ by similar arguments. The above two paths are highlighted in green in Fig. 2. Another set of likely pathways (light blue in Fig. 2) ends on $^1G^e$: $(0,0)^1S^e \rightarrow (15,15)^1P^o \rightarrow (15,16)^1G^e$

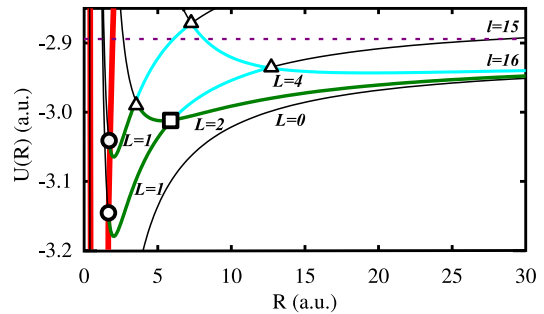


FIG. 2: (Color online) Diabatic dressed potentials for He in a three color field (ω , 13ω , and 15ω). Only the most significant curves and crossing are shown, where a circle indicates a single large-photon crossing; a square a 1-IR photon crossing; and a triangle, a 3-IR photon crossing. The dashed line indicates the energy of the system, which is approximately conserved in this representation.

and $(0,0)^1S^e \rightarrow (13,13)^1P^o \rightarrow (13,16)^1G^e$. Other outcomes are certainly possible and will occur with some probability. The goal of this kind of analysis, though, is to try to identify the main routes to a given final state. Since there exists more than one pathway to this lowest above-threshold ionization (ATI) peak, interference will occur. Similar considerations show that there are generally multiple paths to ionization for each higher ATI peak $l=17,18,19,\dots$ opening up the possibility of control.

In this manner, our formulation of the problem lets us learn a considerable amount about controlling this interference without solving the time-dependent problem. To see explicitly how these pathways interfere, we can derive an expression for any physical observable using Eq. (3). In particular, for the He IR+APT photoelectron spectrum discussed above, we obtain

$$\frac{dP_{\text{ion}}}{dE} = \sum_L \sum_{m,m'} \sum_{l,l'} e^{i(m-m')\omega\tau} e^{i(l'-l)\varphi_1} \times \langle EL|F_{mL}\rangle \langle EL|F_{m'l'L}\rangle^*, \quad (6)$$

where $|EL\rangle$ is an energy-normalized continuum state with asymptotic kinetic energy E and $F_{mL} = e^{-il\omega t} G_{mL}$. All of the τ and φ_1 dependence is displayed analytically since the amplitudes $\langle EL|F_{mL}\rangle$ are independent of these parameters, determining only which pathways will interfere. Equation (6) shows that the delay dependence is determined only by the difference in m , essentially the harmonic order, between two pathways. For the lowest ATI peak discussed above, the final states of two of the pathways identified were $(13,16)^1D^e$ and $(15,16)^1D^e$ for the 13th and 15th harmonics, respectively. Since these have the same final l (net energy absorbed from the field), they will contribute at the same final energy and interfere, resulting in a sinusoidal dependence on $\omega\tau$ with period π since $|m-m'|=2$. This π periodicity in the ionization yield is exactly what was observed in both the

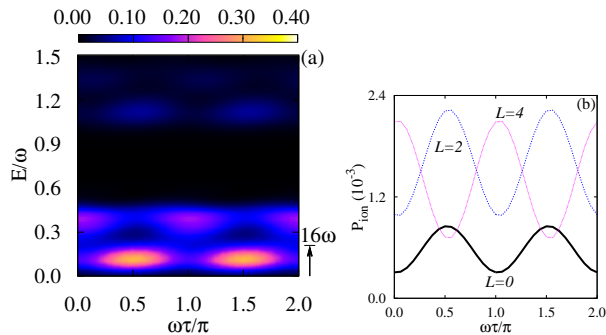


FIG. 3: (Color online) (a) Calculated photoelectron spectrum for an 800 nm IR pulse with $I_1 = 5.0 \times 10^{12}$ W/cm² and $I_{13} = I_{15} = 0.1I_1$. (b) Ionization probability as a function of delay for $L=0, 2$, and 4 .

experiment and numerical results presented in [5, 6]. In general, the periodicity in $\omega\tau$ will be given by $2\pi/|m-m'|$. Thus, if even harmonics had also been included, the periodicity would have been 2π since $|m-m'|$ would equal 1. To see the 2π periodicity, however, one would have to measure a quantity that – unlike the energy spectrum (6) – takes into account interference between different final L s, such as the momentum distribution.

To confirm our analysis, we carried out a full-dimensional numerical solution of the time-dependent Schrödinger equation (1) using the adiabatic hyperspherical representation. Figure 3(a) shows the resulting photoelectron spectrum, again for parameters chosen to be similar to the experiment in [5]. As expected, the calculations show ATI peaks separated by ω . The largest peak is the lowest one (indicated by the arrow), which was discussed above, and the predicted π period of its modulation is clearly seen. A closer look at the 16ω peak reveals that it is split in energy with the lower-energy peak primarily $L=2$ and the higher-energy peak $L=4$ [see Fig. 3(b)]. These details, however, only serve to bolster the value of the dressed potentials we introduced in Fig. 2 since they allowed us to predict that the 16ω peak should be dominated by $L=2$ and 4 . The time-dependent calculations and the dressed potential picture complement each other, providing both quantitative and qualitative understanding of these processes.

This discussion hardly exhausts the insight that can be gleaned from Eq. (6). Another example is the fact that the delay τ between IR and APT will not generate a left-right asymmetry along the laser polarization since all of the L s corresponding to a given ATI peak are either even or odd (with only odd harmonics in the APT). An exception to this statement occurs for broad bandwidth pulses since the interference between even and odd L s necessary for asymmetry can be produced in the overlap of neighboring ATI peaks. Of course, the CEP will also contribute to the asymmetry in this case.

In this Letter, we have presented a general, exact representation for the interaction of multicolor laser pulses

with atoms and molecules upon which a relatively simple interpretive, predictive picture can be built. In the process, we introduced dressed potentials for He — again based on a rigorous derivation — that confer many of the benefits such potentials have provided for molecules on the atomic problem. We have also shown that control via the CEP and the delay between multicolor fields, IR+APT in particular, are conceptually equivalent, being the result of interference between different multiphoton pathways between the initial and final states. Experiments exercising this control are thus quite properly thought of as coherent control.

This work is supported by the Chemical Sciences, Geoscience, and Biosciences Division, Office for Basic Energy Sciences, Office of Science, U.S. Department of Energy.

-
- [1] P. B. Corkum and Z. Chang, *Opt. and Pho. News* **19**, 25 (2008).
 - [2] F. Krausz and M. Ivanov, *Rev. Mod. Phys.* **81**, 163 (2009).
 - [3] M. Hentschel *et al.*, *Nature* **414**, 509 (2001).
 - [4] P. M. Paul *et al.*, *Science* **292**, 1689 (2001).
 - [5] P. Johnsson *et al.*, *Phys. Rev. Lett.* **99**, 233001 (2007).
 - [6] P. Ranitovic *et al.*, *New J. Phys.* (submitted).
 - [7] O. Guyétand *et al.*, *J. Phys. B: At. Mol. Opt. Phys* **38**, L357 (2005).
 - [8] O. Guyétand *et al.*, *J. Phys. B: At. Mol. Opt. Phys* **41**, 051002 (2008).
 - [9] P. Johnsson *et al.*, *Phys. Rev. Lett.* **95**, 013001 (2005).
 - [10] J. Mauritsson *et al.*, *Phys. Rev. Lett.* **100**, 073003 (2008).
 - [11] A. Maquet and R. Taïeb, *J. Mod Opt.* **54**, 1847 (2007).
 - [12] M. Meyer *et al.*, *Phys. Rev. A* **74**, 011401(R) (2006).
 - [13] P. Riviere *et al.*, *New J. Phys.* **11**, 053011 (2009).
 - [14] V. Roudnev and B. D. Esry, *Phys. Rev. Lett.* **99**, 220406 (2007).
 - [15] J.J.Hua and B. D. Esry, *J. Phys. B: At. Mol. Opt. Phys* **42**, 085601 (2009).
 - [16] J. M. Dahlström *et al.*, *Phys. Rev. A* **80**, 033836 (2009).
 - [17] N. Dudovich *et al.*, *Nat. Phys.* **2**, 781 (2006).
 - [18] P. Brumer and M. Shapiro, *Annu. Rev. of Phys. Chem.* **43**, 257 (1992).
 - [19] E. Charron, A. Giusti-Suzor, and F. H. Mies, *Phys. Rev. Lett.* **71**, 692 (1993).
 - [20] E. Charron, A. Giusti-Suzor, and F. H. Mies, *Phys. Rev. Lett.* **75**, 2815 (1995).
 - [21] T. T. Nguyen-Dang *et al.*, *Phys. Rev. A* **71**, 023403 (2005).
 - [22] S.-I. Chu and D. A. Telnov, *Phys. Rep.* **390**, 1 (2004).
 - [23] X. Guan, X. M. Tong, and Shih-I Chu, *Phys. Rev. A* **73**, 023403 (2006).
 - [24] C. D. Lin, *Adv. At. Mol. Opt. Phy.* **22**, 77 (1986).
 - [25] C. de Boor, *A practical guide to splines* (Springer-Verlag, 1978).
 - [26] J. H. Posthumus, *Rep. Prog. Phys.* **67**, 623 (2004).
 - [27] A. Giusti-Suzor *et al.*, *J. Phys. B: At. Mol. Opt. Phys* **28**, 309 (1995).
 - [28] B. D. Esry *et al.*, *Phys. Rev. Lett.* **97**, 013003 (2006).